

# GP3D: Generalized Pose Estimation in 3D Point Clouds: A case study on bin picking

1<sup>st</sup> Frederik Hagelskjær

SDU Robotics

University of Southern Denmark

Odense, Denmark

frhag@mmmi.sdu.dk

**Abstract**—In this paper, we present GP3D, a novel network for generalized pose estimation in 3D point clouds. The method generalizes to new objects by using both the scene point cloud and the object point cloud with keypoint indexes as input. The network is trained to match the object keypoints to scene points.

To address the pose estimation of novel objects we also present a new approach for training pose estimation. The typical solution is a single model trained for pose estimation of a specific object in any scenario. This has several drawbacks: training a model for each object is time-consuming, energy consuming, and by excluding the scenario information the task becomes more difficult.

In this paper, we present the opposite solution; a scenario-specific pose estimation method for novel objects that do not require retraining. The network is trained on 1500 objects and is able to learn a generalized solution. We demonstrate that the network is able to correctly predict novel objects, and demonstrate the ability of the network to perform outside of the trained class. We believe that the demonstrated method is a valuable solution for many real-world scenarios. Code and trained network will be made available after publication.

**Index Terms**—pose estimation, point cloud, deep learning

## I. INTRODUCTION

Pose estimation enables much greater flexibility in robotics. New objects can be manipulated without the need for mechanical fixtures or teaching specific robot positions. This enables a more adaptive production with a shorter changeover time and faster adaptation to production demands. However, the set-up of computer vision set-ups can itself be a very time-consuming task [6]. There is, therefore, great interest in pose estimation solutions with simple set-ups. Deep learning has allowed learning the specifics of the object and the scenario thus giving much better performance than human fine-tuning [10], [18]. However, collecting the data for training the deep neural networks can be very time-consuming, thereby limiting the usability. To avoid this data collection, the use of synthetic data has gained widespread use [10]. But, this introduces a domain gap between the real world and the training data, which is often handled by adding large amounts of domain randomization during training [18]. In this solution a single model is trained for one object adapted to any scenario. However, we believe that by utilizing the scenario information a single model can be trained for multiple objects. For many set-ups this much better fit the tasks at hand. It allow us to train on real data as training is not required for new objects. New

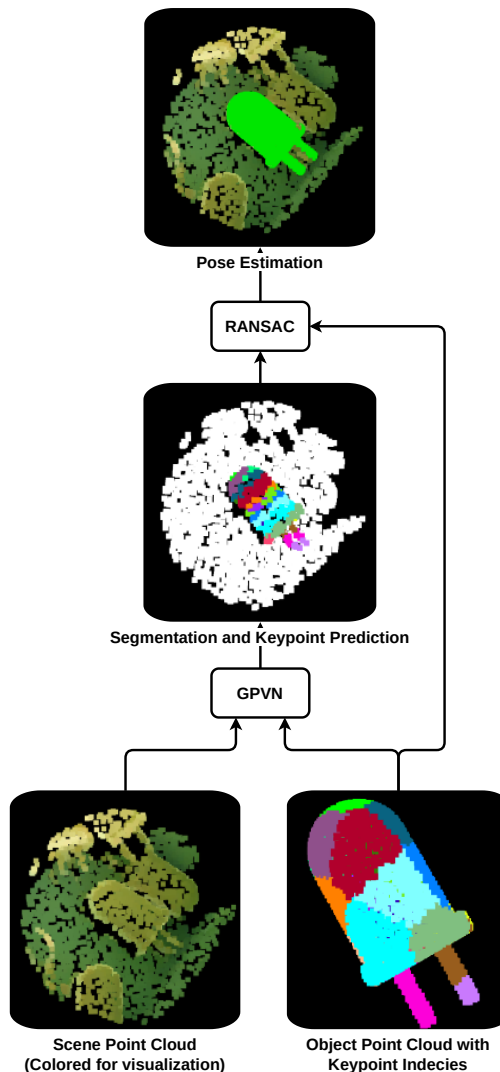


Fig. 1. Illustration of the pose estimation method. The input to the network is a scene point cloud and an object point cloud with keypoints spread over the object. The output of the network is object segmentation and keypoint votes. Notice how the rotational symmetry makes a striped pattern of keypoint predictions. Finally these votes are used in RANSAC for pose estimation.

objects can be introduced faster as training is not required, and the power consumption for training will be removed. An example is robotic work-cells where the scenario is constant while new objects are introduced. In this paper we focus on the

task of bin picking with homogeneous bins, which is a difficult challenge that often occurs in industry. The homogeneous bin, also removes the need for object detection and allow us to only focus on pose estimation.

We recognize that the general approach as shown in e.g. [18] has huge importance, but also state it is not the best solution for all tasks. In this paper we show that generalized pose estimation can show very good performance when restricting the scenario.

We believe that these results invite further research into this topic, as more flexible robotic set-ups with lower power consumption is an important topic.

## II. RELATED WORKS

Visual pose estimation is an important topic, and many different approaches have been developed.

**Classic Pose Estimation:** The classic pose estimation approach is based on matching features between the scene and object, and computing the pose by e.g. RANSAC [2]. The matches are computed using handcrafted features, which is generally computed in 3D point clouds. A huge amount of handcrafted features have been developed [4], with Fast Point Feature Histograms (FPFH) [16] being one of the best performing features.

**Deep Learning Based:** Generally deep learning based methods are based on color information [10], [18]. This is possibly a result of many deep learning based methods developed for this space, with huge pre-trained networks available. These methods have vastly outperformed the classical methods, however, a network is often trained per object [10], [18]. Deep learning for pose estimation has also been performed in point clouds with methods such as PointVoteNet [5]. We base our method on PointVoteNet, but only train a single network for all objects.

**Generalized Pose Estimation:** Several approaches have been developed for generalized pose estimation. As in the deep learning based pose estimation, the field of generalized pose estimation is also dominated by color-based methods [8], [12], [17]. The general approach for these methods is to match templates of the object with the real image. These templates can either be generated synthetically as in [14] or with a few real images as in FS6D [8]. The same approach have also been used for tracking of unknown objects [13]. MegaPose6D [12] is a notable example where the network is trained on a huge dataset with 2 million images. The method most similar to ours is a point cloud based method [3]. It also uses the object model as input. However, several differences are present compared with our approach; the method includes color information, it does not limit the scenario and thus does not obtain the increased performance from this, and it does not separate the object and scene features.

## III. METHOD

The developed method is based on DGCNN [19] and bears a similarity to a similar pose estimation network [5]. Point clouds are well suited for industrial objects as precise CAD

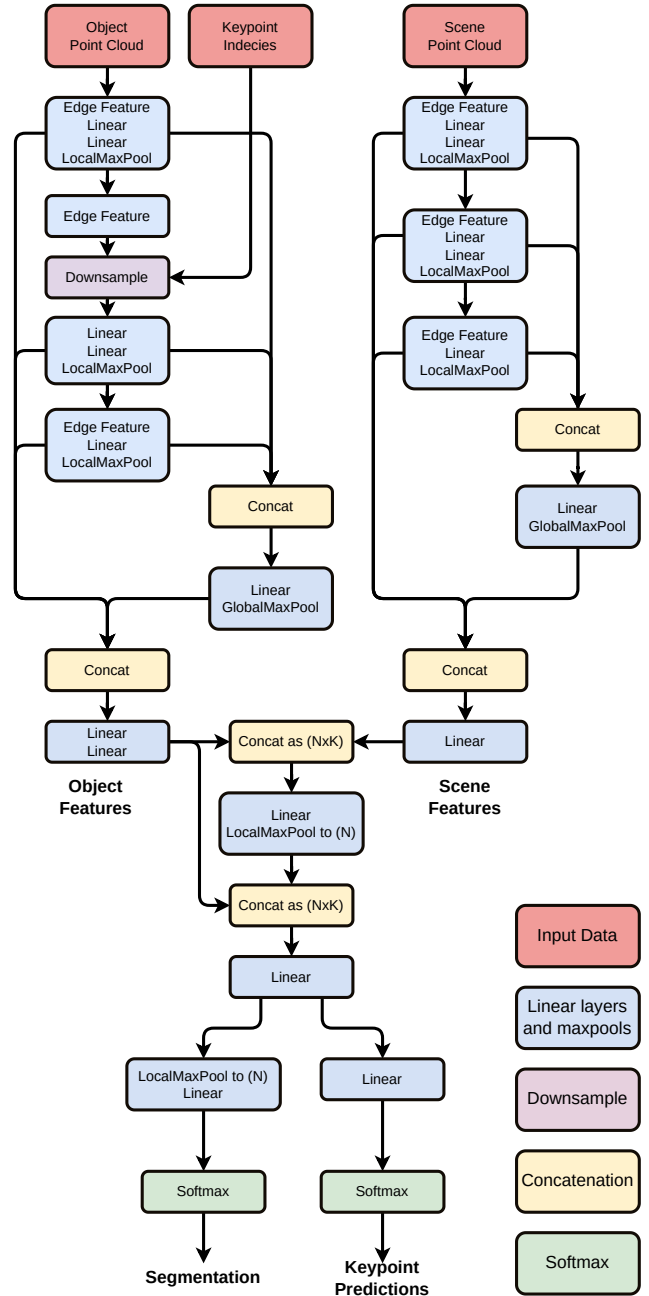


Fig. 2. The network structure for the developed method. Initially features are computed independently for the object and the scene. This allow us to compute the object features a single time and match it with multiple scene point clouds. The "Edge Feature" is specific to DGCNN and computes and concatenates neighbor points.

models are generally available, but color and surface is rarely available. Compared with PointVoteNet we introduce several differences.

Instead of learning the prediction of cad model keypoints directly in the network, as in previous methods, we instead train the network to match keypoint features from the object to the scene point cloud. The network structure is shown in Fig. 2. Initially the object and keypoint features are com-

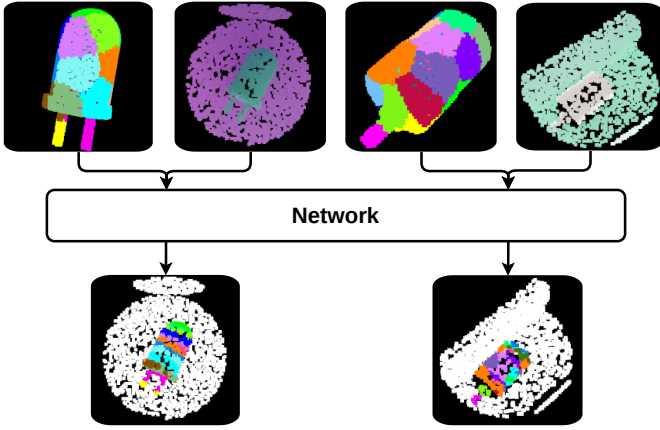


Fig. 3. An illustration of the networks ability to correctly match keypoints from multiple objects. Both objects are unknown to the object, with the right object being out of class.

puted independently using the standard feed-forward part of DGCNN. However, as only the keypoints from the object point cloud is needed the object point cloud is down-sampled to the twenty keypoints after the second neighbor computation in the DGCNN. As the number of neighbors is set to the same as the number of keypoints, all keypoints include information about the other.

After both object and scene features are computed they are joined together to create a matrix of length  $(n * k)$ , where  $n$  is the number of point and  $k$  is the number of keypoints. A linear layer then processes each join independently and a local maxpool reduces the matrix to length  $(n)$ , combining all keypoint information for the scene point. The object features are then joined again and a linear layer computes features per keypoint-scene point pair. By applying a softmax the prediction for each keypoint is computed. To compute the segmentation a local maxpool is applied followed by a linear layer. In Fig. 3 the networks ability to correctly classify keypoints for different objects is shown.

Finally, RANSAC is used with the segmentation and keypoint predictions to compute the final object pose. We employ the vote threshold as in [5] to allow multiple predictions at a single point. The vote threshold is set to 0.7.

#### A. Generating scene data

As the scenario is homogeneous bin-picking the detection is vastly simplified. As the bin position is known beforehand, and the contents are homogeneous, any point belongs to an object. Thus we can randomly sample point a point, and this point will belong to the object. By then extracting using a radius set to the object model diagonal, all points in the scene belonging to the object will be obtained. The point cloud is then centered around the sampled point to allow for instance segmentation. The scene point clouds are generated using BlenderProc [1].

#### B. Generating object data

The object point clouds is generated using Poisson sampling to obtain 2048 evenly sampled points on the surface.

Farthest point sampling is then used to obtain the keypoints spread evenly on the object. During training the keypoints are continuously re-computed with random initialization, to avoid the network over-fitting to a specific combination.

#### C. Computing object features off-line

As shown in Fig. 2 the features computed from object point cloud are independent of the features computed from the scene point cloud. This is opposed to [3]. This allow us to use the same object feature for multiple pose estimations. The object features can also be computed offline to reduce the run-time and the computational cost.

## IV. EXPERIMENTS

To test the developed method several experiments are performed. A single network is trained and tested for all the experiments. The network is trained on 1500 free cad models from an online database of electronic components<sup>1</sup>. Fifty models are used as validation to test the networks ability on unseen objects. The method is also tested on novel objects. Seven electrical components from a different database are tested [7]. The seven test objects are shown at the top of Fig. 4. Additionally we test the ability of the network on industrial objects from the WRS [21] dataset. On this dataset we show the networks ability to generalize to other objects outside of the training scope. The objects from the WRS dataset are shown in the bottom of Fig. 4. All point cloud processing and pose estimation is performed using the Open3D framework, [22]. The network processing was performed using PyTorch [15].

#### A. Network Training

The 1500 components are split into a 1450/50 train-validation dataset. During each epoch we generate 160 point clouds for each component. Thus each training epoch consists of 232000 point clouds. The network is trained with a batch size of 14, 7 on each GPU, using the Adam optimizer [11], with an initial learning rate of 0.0001. We use a step scheduler with a step size of 20 and the gamma parameter set to 0.7. The loss is calculated with cross entropy using a 0.2/0.8 split for segmentation and keypoint loss. For the keypoint loss only points belonging to the object is used.

To generalize the network Group Norm [20] with group size 32 is used after each linear layer. Group Norm is used as opposed to Batch Norm as a result of the small batch size. Dropout is used for the object features, as the network should not overfit to a specific part of the object, and is used after the to concurrent linear layers. The dropout is set to 40 %, used after the last two linear layers of the object feature and the first two of the combined feature. Additionally, up to 0.75 % Gaussian noise is applied to the object and scene point clouds, and 10 % position shift is applied to the object point cloud.

The network was trained on a PC environment with two NVIDIA GeForce RTX 2080 GPUs. The network was trained for 120 epochs lasting approximately six days (141 hours).

<sup>1</sup>[https://www.pcb-3d.com/membership\\_type/free/](https://www.pcb-3d.com/membership_type/free/)

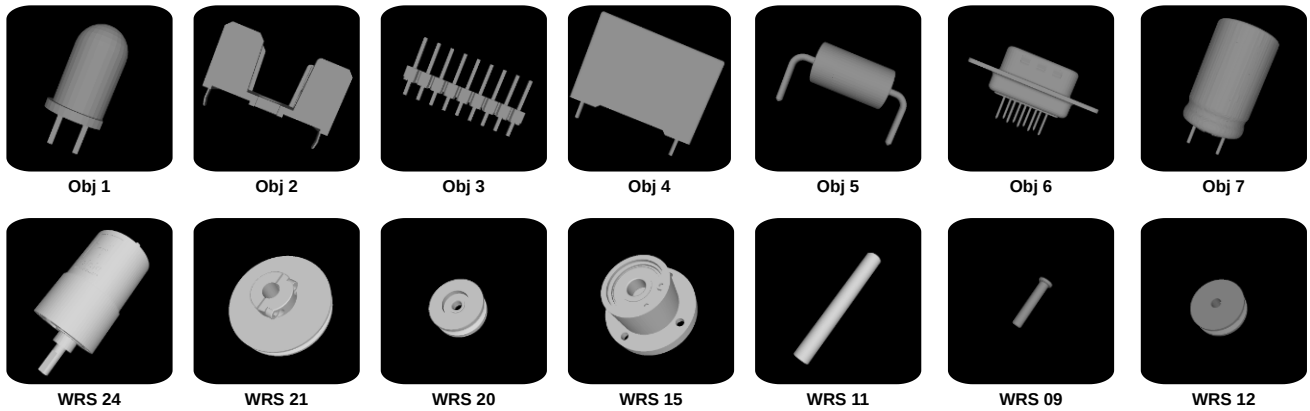


Fig. 4. The seven electronic components used for testing, along with the seven components from the WRS dataset used for out of class testing.

Split	Train (w/ gen.)	Train (w/o gen.)	Val	Test
Loss	1.59	1.42	1.33	1.57
Seg. Acc	0.98	0.97	0.96	0.95
Key. Acc	0.27	0.29	0.31	0.25

TABLE I

THE LOSS AND ACCURACY OF THE NETWORK ON THE DIFFERENT DATASETS. RESULTS ARE SHOWN FOR THE TRAINING DATA BOTH WITH AND WITHOUT THE GENERALIZATION APPLIED DURING TRAINING.

Object	1	2	3	4	5	6	7
Loss	1.50	2.03	1.12	1.53	1.42	1.84	1.53
Seg. Acc	0.99	0.81	0.98	0.98	0.95	0.97	0.99
Key. Acc	0.24	0.16	0.43	0.29	0.31	0.22	0.22

TABLE II

LOSS AND ACCURACY OF EACH OF THE INDIVIDUAL TEST OBJECTS.

### B. Training and test performance

The performance for the trained networks is shown in Tab. I. Performance is shown for both the loss, segmentation accuracy, and keypoint accuracy. We present the training performance both with and without generalization. The network does not appear to overfit to the training data, and actually shows better performance on the validation set. For the test data with electronic objects not from the same dataset, the network performs well with a slightly lower performance. As the objects are symmetric to varying levels, the keypoint accuracy despite being low, still gives good pose estimations. This is seen in Fig. 1, where the symmetry of the object results in striped matching of keypoints. However, these matches are still very useful for the pose estimation.

### C. Performance for each component

To analyze the network, performance for each component is shown in Tab. II. The two objects with the highest performance are "3" and "5". These two objects are both very similar to objects in the training data. The most challenging object is "2". The split between the two parts of the object makes it very dissimilar to the training data. The other components perform very well, especially for the segmentation task.

Object	1	2	3	4	5	6	7
Ours	0.95	0.82	0.99	0.77	0.91	0.90	0.92
Classic	0.55	0.62	0.61	0.30	0.36	0.67	0.51
Ours 1% noise	0.93	0.79	0.99	0.74	0.86	0.88	0.90
Classic 1% noise	0.43	0.57	0.50	0.25	0.31	0.66	0.40
Ours 5% noise	0.55	0.60	0.91	0.62	0.83	0.82	0.53
Classic 5% noise	0.30	0.54	0.45	0.20	0.43	0.56	0.25

TABLE III

POSE ESTIMATION ACCURACY FOR EACH OF THE TEST COMPONENTS. A COMPARISON WITH CLASSIC POSE ESTIMATION IS SHOWN. RESULTS ARE ALSO SHOWN WITH NOISE ADDED TO THE SCENE POINT CLOUD.

### D. Pose Estimation Performance

To test the pose estimation ability of the network we compare it with a classic pose estimation method. The classic pose estimation method is FPFH [16] with RANSAC [2]. The performance is measured by the ADD-S score, as it is well suited for the symmetric objects in our dataset [9]. To further test the robustness of the system, varying levels of noise is added to the point clouds. The results are shown in Tab. III. It can be seen that our method outperforms the classic method for all objects. When adding noise the difference becomes even more pronounced. However, for the 5% noise the performance also drops significantly for our method.

### E. Testing out of class

The WRS dataset consists of industrial objects, such as motors and pulleys. The objects were used for the WRS assembly challenge held in 2018 [21]. We have chosen they represent an industrial challenge and because of the variety. The results of the network performance and pose estimation is shown in Tab. IV. It is seen that our developed method obtains very good performance on these objects that appear quite different than the training dataset. As seen in Fig. 5, because the objects are quite symmetric, the pose estimation succeeds even though the keypoints prediction is not correct.

### F. Run-time

The run-time of the network was tested both with and without computing the object features at run-time. With the object features computed at run-time the processing lasts

Object	24	21	20	15	11	09	12
Pose Est.	1.00	0.99	0.90	0.91	0.93	0.93	0.96

TABLE IV

THE POSE ESTIMATION ACCURACY OF OUR METHOD ON THE UNSEEN WRS DATASET.

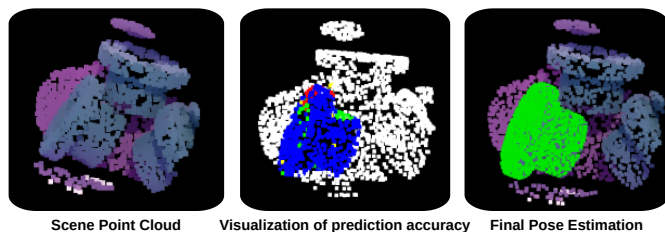


Fig. 5. Visualization of the pose estimation accuracy despite low keypoint precision. In the central figure the prediction accuracy of the network is visualized. "White" represents correctly predicted background, "red" false negatives and "yellow" false positives. "Blue" is correctly predicted segmentation of the object, but wrong keypoints and "green" is both correct segmentation and keypoint prediction. To the right the pose estimation is shown.

14.9 ms. While by pre-computing the features the run-time is only 7.9 ms. The separation of object and scene feature computations is thus a significant speed-up.

However, for the full system the run-time is currently 84.7 ms. This is mainly related to the RANSAC search, which would be a focus to replace.

## V. CONCLUSION

In this paper we have presented a novel method for generalized pose estimation. The method consists of a novel network structure and a scenario specific approach. The method show very good generalizability across different objects, even with out of class objects. This proves the validity of creating object independent networks for specific scenarios, which can be useful for many real world applications.

In future work, it will be very interesting to test the method with real data, both for training and testing. Additionally, the network could be adapted to perform full pose estimation to simplify the pipeline and improve the run-time. The objects from the MegaPose6D [12] dataset could also be used to diversify the object types, and test on benchmark datasets.

## REFERENCES

- [1] Maximilian Denninger, Martin Sundermeyer, Dominik Winkelbauer, Youssef Zidan, Dmitry Olefir, Mohamad Elbadrawy, Ahsan Lodhi, and Harinandan Katam. Blenderproc. *arXiv preprint arXiv:1911.01911*, 2019.
- [2] Martin A Fischler and Robert C Bolles. Random sample consensus: a paradigm for model fitting with applications to image analysis and automated cartography. *Communications of the ACM*, 24(6):381–395, 1981.
- [3] Minghao Gou, Haolin Pan, Hao-Shu Fang, Ziyuan Liu, Cewu Lu, and Ping Tan. Unseen object 6d pose estimation: a benchmark and baselines. *arXiv preprint arXiv:2206.11808*, 2022.
- [4] Yulan Guo, Mohammed Bennamoun, Ferdous Sohel, Min Lu, Jianwei Wan, and Ngai Ming Kwok. A comprehensive performance evaluation of 3d local feature descriptors. *International Journal of Computer Vision*, 116:66–89, 2016.
- [5] Frederik Hagelskjær and Anders Glent Buch. Pointvotenet: Accurate object detection and 6 dof pose estimation in point clouds. In *2020 IEEE International Conference on Image Processing (ICIP)*, pages 2641–2645. IEEE, 2020.
- [6] Frederik Hagelskjær, Anders Glent Buch, and Norbert Krüger. Does vision work well enough for industry? In *VISIGRAPP (4: VISAPP)*, pages 198–205, 2018.
- [7] Frederik Hagelskjær and Dirk Kraft. In-hand pose estimation and pin inspection for insertion of through-hole components. In *2022 IEEE 18th International Conference on Automation Science and Engineering (CASE)*, pages 382–389. IEEE, 2022.
- [8] Yisheng He, Yao Wang, Haoqiang Fan, Jian Sun, and Qifeng Chen. Fs6d: Few-shot 6d pose estimation of novel objects. In *Proceedings of the IEEE/CVF Conference on Computer Vision and Pattern Recognition*, pages 6814–6824, 2022.
- [9] Stefan Hinterstoisser, Vincent Lepetit, Slobodan Ilic, Stefan Holzer, Gary Bradski, Kurt Konolige, and Nassir Navab. Model based training, detection and pose estimation of texture-less 3d objects in heavily cluttered scenes. In *Computer Vision—ACCV 2012: 11th Asian Conference on Computer Vision, Daejeon, Korea, November 5-9, 2012, Revised Selected Papers, Part I 11*, pages 548–562. Springer, 2013.
- [10] Tomáš Hodaň, Martin Sundermeyer, Bertram Drost, Yann Labbé, Eric Brachmann, Frank Michel, Carsten Rother, and Jiří Matas. Bop challenge 2020 on 6d object localization. In *Computer Vision—ECCV 2020 Workshops: Glasgow, UK, August 23–28, 2020, Proceedings, Part II 16*, pages 577–594. Springer, 2020.
- [11] Diederik P Kingma and Jimmy Ba. Adam: A method for stochastic optimization. *arXiv preprint arXiv:1412.6980*, 2014.
- [12] Yann Labbé, Lucas Manuelli, Arsalan Mousavian, Stephen Tyree, Stan Birchfield, Jonathan Tremblay, Justin Carpenter, Mathieu Aubry, Dieter Fox, and Josef Sivic. Megapose: 6d pose estimation of novel objects via render & compare. *arXiv preprint arXiv:2212.06870*, 2022.
- [13] Van Nguyen Nguyen, Yuming Du, Yang Xiao, Michael Ramamonjisoa, and Vincent Lepetit. Pizza: A powerful image-only zero-shot zero-cad approach to 6 dof tracking. *arXiv preprint arXiv:2209.07589*, 2022.
- [14] Van Nguyen Nguyen, Yinlin Hu, Yang Xiao, Mathieu Salzmann, and Vincent Lepetit. Templates for 3d object pose estimation revisited: generalization to new objects and robustness to occlusions. In *Proceedings of the IEEE/CVF Conference on Computer Vision and Pattern Recognition*, pages 6771–6780, 2022.
- [15] Adam Paszke, Sam Gross, Francisco Massa, Adam Lerer, James Bradbury, Gregory Chanan, Trevor Killeen, Zeming Lin, Natalia Gimelshein, Luca Antiga, Alban Desmaison, Andreas Kopf, Edward Yang, Zachary DeVito, Martin Raison, Alykhan Tejani, Sasank Chilamkurthy, Benoit Steiner, Lu Fang, Junjie Bai, and Soumith Chintala. PyTorch: An Imperative Style, High-Performance Deep Learning Library. In H. Wallach, H. Larochelle, A. Beygelzimer, F. d’Alché Buc, E. Fox, and R. Garnett, editors, *Advances in Neural Information Processing Systems 32*, pages 8024–8035. Curran Associates, Inc., 2019.
- [16] Radu Bogdan Rusu, Nico Blodow, and Michael Beetz. Fast point feature histograms (fpfh) for 3d registration. In *2009 IEEE international conference on robotics and automation*, pages 3212–3217. IEEE, 2009.
- [17] Ivan Shugurov, Fu Li, Benjamin Busam, and Slobodan Ilic. Osop: a multi-stage one shot object pose estimation framework. In *Proceedings of the IEEE/CVF Conference on Computer Vision and Pattern Recognition*, pages 6835–6844, 2022.
- [18] Martin Sundermeyer, Tomas Hodan, Yann Labbe, Gu Wang, Eric Brachmann, Bertram Drost, Carsten Rother, and Jiri Matas. Bop challenge 2022 on detection, segmentation and pose estimation of specific rigid objects. *arXiv preprint arXiv:2302.13075*, 2023.
- [19] Yue Wang, Yongbin Sun, Ziwei Liu, Sanjay E Sarma, Michael M Bronstein, and Justin M Solomon. Dynamic graph cnn for learning on point clouds. *Acm Transactions On Graphics (tog)*, 38(5):1–12, 2019.
- [20] Yuxin Wu and Kaiming He. Group normalization. In *Proceedings of the European conference on computer vision (ECCV)*, pages 3–19, 2018.
- [21] Yasuyoshi Yokokohji, Yoshihiro Kawai, Mizuho Shibata, Yasumichi Aiyama, Shinya Kotosaka, Wataru Uemura, Akio Noda, Hiroki Dobashi, Takeshi Sakaguchi, and Kazuhito Yokoi. Assembly challenge: a robot competition of the industrial robotics category, world robot summit—summary of the pre-competition in 2018. *Advanced Robotics*, 33(17):876–899, 2019.
- [22] Qian-Yi Zhou, Jaesik Park, and Vladlen Koltun. Open3D: A modern library for 3D data processing. *arXiv:1801.09847*, 2018.